

See discussions, stats, and author profiles for this publication at: <https://www.researchgate.net/publication/244459379>

# Structural Variation in Diorganotin Dimethylxanthates, $R_2Sn(S_2COMe)_2$ : A Combined Crystallographic and Theoretical Investigation †

ARTICLE in ORGANOMETALLICS · DECEMBER 2000

Impact Factor: 4.13 · DOI: 10.1021/om000717v

---

CITATIONS

37

---

READS

19

5 AUTHORS, INCLUDING:



Mark A. Buntine

Curtin University

108 PUBLICATIONS 1,412 CITATIONS

SEE PROFILE



Edward Tiekink

Sunway Education Group

2,168 PUBLICATIONS 15,122 CITATIONS

SEE PROFILE

# Structural Variation in Diorganotin Dimethylxanthates, $R_2Sn(S_2COMe)_2$ : A Combined Crystallographic and Theoretical Investigation<sup>†</sup>

Mohamed Ismail Mohamed-Ibrahim and Suan See Chee

Chemical Sciences Programme, School of Distance Education, Universiti Sains Malaysia,  
11800 Penang, Malaysia

Mark A. Buntine, Michael J. Cox, and Edward R. T. Tiekink\*

Department of Chemistry, The University of Adelaide, South Australia 5005, Australia

Received August 16, 2000

The crystal and molecular structures of three  $R_2Sn(S_2COMe)_2$  compounds have been determined and show that the tin atom in each case exists in a distorted trapezoidal bipyramidal geometry with the tin-bound organo substituents lying over the longer edge of the trapezoidal plane. For  $Me_2Sn(S_2COMe)_2$ , one of the xanthate ligands coordinates via both sulfur atoms (S-,S- chelation) but the other uses one sulfur and the oxygen atom in coordination to tin (S-,O- chelation). More conventional geometries, with S-,S- chelation only, are found for  $Ph(Me)Sn(S_2COMe)_2$  and  $Ph_2Sn(S_2COMe)_2$ . Theoretical predictions of the isolated molecular structures have been calculated using ab initio and density functional theories (all with the 3-21G\*\* basis set) and reveal a different arrangement of the ligand donor set for each compound, i.e., one featuring both ligands with S-,O- chelation. Differences between the single-molecule and solid-state structures are ascribed to the influence of intermolecular interactions on the molecular geometries in the solid state.

## Introduction

Recent bibliographic reviews of the structural chemistry of organotin systems, as determined by X-ray crystallography, have shown that remarkable diversity in structure may sometimes be observed even when only small changes in chemistry exist.<sup>1,2</sup> Thus, for the diorganotin bis(1,1-dithiolates) [e.g., 1,1-dithiolate =  $^-S_2CNR'_2$  (dithiocarbamate),  $^-S_2COR$  (xanthate),  $^-S_2P(OR)_2$  (dithiophosphate), etc.] four structural motifs are found,<sup>2</sup> as shown in Figure 1. The majority of structures adopt motif **A**, which features a skew-trapezoidal bipyramidal geometry.<sup>2,3</sup> The trapezoidal plane is defined by four sulfur atoms derived from two asymmetrically coordinating 1,1-dithiolate ligands and the tin-bound organo substituents are orientated over the weakly bound sulfur atoms so that the C–Sn–C angles lie in the range 121.8(5)–150.2(4)°.<sup>2</sup> In motif **B**, the organo substituents occupy mutually cis positions so that the coordination geometry is best described as distorted octahedral.<sup>4–7</sup> A distorted octahedral geometry is also found in motif **C**, where the organo substituents occupy

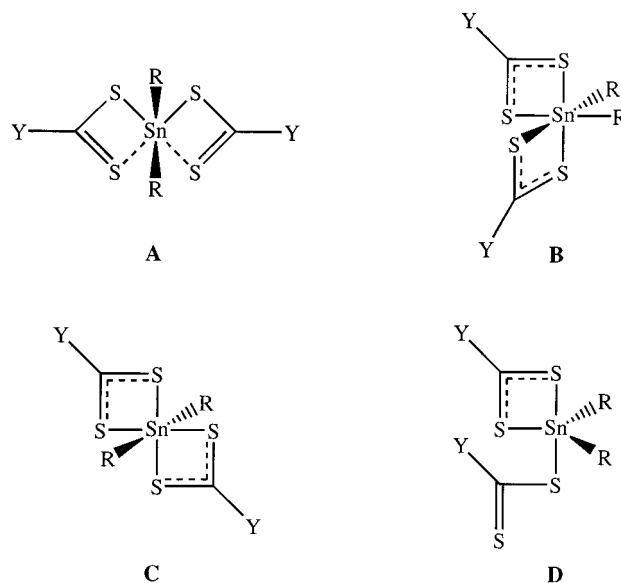


**Figure 1.** Different structural motifs for  $R_2Sn(S_2CY)_2$  (see text).

mutually trans positions.<sup>8</sup> Finally, a reduced coordination number is found in motif **D**, where the tin atom exists in a distorted trigonal bipyramidal geometry owing to the presence of a monodentate dithiocarbamate ligand.<sup>9</sup> The reasons for the adoption of the different

<sup>†</sup> Dedicated to the memory of George Winter.

(1) Tiekink, E. R. T. *Trends in Organomet. Chem.* **1994**, 1, 71; *Appl. Organomet. Chem.* **1991**, 5, 1.

(2) Tiekink, E. R. T. *Main Group Metal Chem.* **1992**, 15, 161.

(3) Hall, V. J.; Tiekink, E. R. T. *Main Group Met. Chem.* **1998**, 21, 245.

(4) Lindley, P. F.; Carr, P. *J. Cryst. Mol. Struct.* **1974**, 4, 173.

(5) Alcock, N. W.; Culver, J.; Roe, S. M. *J. Chem. Soc., Dalton Trans.* **1992**, 1477.

(6) Hook, J. M.; Linahan, B. M.; Taylor, R. L.; Tiekink, E. R. T.; van Gorkom, L.; Webster, L. K. *Main Group Met. Chem.* **1994**, 17, 293.

(7) Hall, V. J.; Tiekink, E. R. T. *Main Group Met. Chem.* **1995**, 18, 611.

(8) Molloy, K. C.; Hossain, M. B.; van der Helm, D.; Zuckerman, J. J.; Haiduc, I. *Inorg. Chem.* **1980**, 19, 75.

(9) Kim, K.; Ibers, J. A.; Jung, O.-S.; Sohn, Y. S. *Acta Crystallogr., Sect. C* **1987**, 43, 2317.

structural motifs have yet to be ascertained. These may relate to electronic, steric, or crystal packing effects or some combination of these. Clearly, systematic investigations are required in order to determine the relative importance of these factors. In this contribution an examination of a series of  $R_2Sn(S_2COMe)_2$  structures employing both experimental (i.e., crystallography) and theoretical (i.e., ab initio molecular orbital calculations) methods is described.

Recent investigations have shown that such a combined crystallographic/theoretical protocol proves very useful in examining the relative importance of electronic, steric, and crystal packing effects on molecular structure in organotin systems<sup>10–12</sup> and indeed in other systems containing heavy elements.<sup>13–15</sup> The key result of such studies has been the demonstration that the often ignored crystal packing effects, i.e., intermolecular forces, do indeed exert a significant influence on coordination geometry as well as on the derived interatomic parameters. For example, calculations have repeatedly shown that nonsymmetric structures converge to symmetric structures in the absence of solid-state effects.<sup>10–12</sup> In the same way, calculations on polymorphs invariably demonstrate that differences in conformation and/or bond distances can be related to crystal packing effects. Further, nonsystematic variations in derived interatomic parameters found in the solid state no longer pertain in the theoretical gas-phase structures.<sup>10–12</sup> In other words, it would seem that variations in geometric parameters are greater than those indicated by conventional crystallographic errors. In this context, it is important to note that comparable variations in geometric parameters have been noted in certain transition metal systems.<sup>16,17</sup> As a continuation of studies examining the role of crystal packing effects on molecular geometry in organotin systems, the present report describes an investigation of the structural characteristics of three  $R_2Sn(S_2COMe)_2$  compounds where structural diversity and nonsystematic variations in derived interatomic parameters are found in the solid state.

## Results and Discussion

**Solid-State Structures.** The structure of  $Me_2Sn(S_2COMe)_2$  (**1**) is shown in Figure 2a, and selected interatomic parameters are collected in Table 1. The tin atom in **1** is coordinated by two methyl groups and two methylxanthate ligands, with the latter adopting different coordination modes. The first xanthate ligand is chelating but forms asymmetric Sn–S bond distances of 2.482(1) Å and 2.900(1) Å, respectively. The weaker Sn–S(2) distance is well within the sum of the van der Waals radii for the Sn and S atoms of 4.0 Å.<sup>18</sup> By

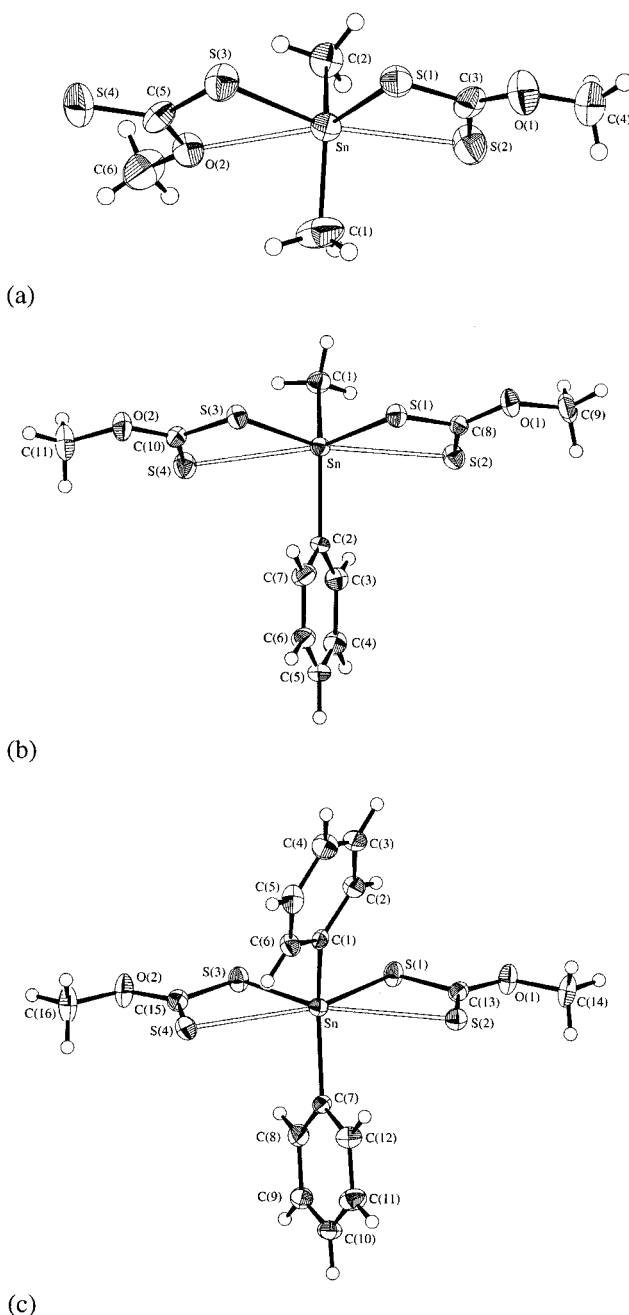


**Figure 2.** Molecular structure and atomic numbering schemes for (a)  $Me_2Sn(S_2COMe)_2$  (**1**), (b)  $Ph(Me)Sn(S_2COMe)_2$  (**2**), and (c)  $Ph_2Sn(S_2COMe)_2$  (**3**).

contrast, to a first approximation, the second xanthate ligand coordinates in the monodentate mode forming a Sn–S(3) distance of 2.538(2) Å. Rather than the S(4) atom being in close proximity to the tin center, there has been a twist about the S(3)–C(5) bond so as to place the O(2) atom at a distance of 2.890(4) Å from tin. This separation is significantly longer than the sum of the covalent radii of these atoms, i.e., 2.13 Å,<sup>18</sup> but at the same time is significantly shorter than the sum of their van der Waals radii of 3.7 Å.<sup>18</sup> Similar S···O modes of coordination have been found in other xanthate systems; however, in all but one example, the M···O distance was close to the respective sum of the van der Waals radii and hence, the M···O interactions were not considered significant; see discussion in refs 19–21. The exception was found in the structure of  $Ph_3Sn(S_2COiPr)_2$ ,<sup>21</sup> where

(10) Buntine, M. A.; Hall, V. J.; Kosovel, F. J.; Tiekink, E. R. T. *J. Phys. Chem. A* **1998**, *102*, 2472.

(11) Buntine, M. A.; Hall, V. J.; Tiekink, E. R. T. *Z. Kristallogr.* **1998**, *213*, 669.

(12) Tiekink, E. R. T.; Hall, V. J.; Buntine, M. A. *Z. Kristallogr.* **1999**, *214*, 242.

(13) Burda, J. V.; Sponer, J.; Hobza, P. *J. Phys. Chem.* **1996**, *100*, 7250.

(14) Jiang, S.; Dasgupta, S.; Blanco, M.; Frazier, R.; Yamaguchi, E. S.; Tang, Y.; Goddard, W. A. *J. Phys. Chem.* **1996**, *100*, 15760.

(15) Stewart, G. M.; Tiekink, E. R. T.; Buntine, M. A. *J. Phys. Chem. A* **1997**, *101*, 5368.

(16) Martin, A.; Orpen, A. G. *J. Am. Chem. Soc.* **1996**, *118*, 1464.

(17) Cotton, F. A.; Yokochi, A. *Inorg. Chem.* **1997**, *36*, 2461.

(18) Bondi, A. *J. Phys. Chem.* **1964**, *68*, 441.

**Table 1. Selected Interatomic Parameters (Å, deg) for Me<sub>2</sub>Sn(S<sub>2</sub>COMe)<sub>2</sub> (1), Ph(Me)Sn(S<sub>2</sub>COMe)<sub>2</sub> (2), and Ph<sub>2</sub>Sn(S<sub>2</sub>COMe)<sub>2</sub> (3) Obtained from Crystallography**

	<b>1</b> X = S(2) Y = O(2)	<b>2</b> X = S(2) Y = S(4)	<b>3</b> X = S(2) Y = S(4)
Sn–S(1)	2.482(1)	2.498(2)	2.498(1)
Sn–X	2.900(1)	3.019(2)	3.126(1)
Sn–S(3)	2.538(2)	2.509(2)	2.502(1)
Sn–Y	2.890(4)	3.089(2)	3.042(1)
Sn–C(1)	2.10(2)	2.107(6)	2.132(4)
Sn–C(2)	2.14(1)	2.123(6)	2.136(3)
S(1)–C	1.733(6)	1.736(6)	1.749(4)
S(2)–C	1.655(6)	1.644(6)	1.658(4)
S(3)–C	1.744(6)	1.725(8)	1.737(5)
S(4)–C	1.609(5)	1.660(7)	1.652(4)
C–O(1)	1.322(7)	1.326(9)	1.313(5)
C–O(2)	1.356(6)	1.323(9)	1.328(6)
S(1)–Sn–X	66.60(4)	64.64(5)	63.34(3)
S(1)–Sn–S(3)	88.67(4)	87.08(6)	85.48(4)
S(1)–Sn–Y	144.06(8)	150.76(5)	149.94(3)
S(1)–Sn–C(1)	114.8(4)	110.7(2)	106.0(1)
S(1)–Sn–C(2)	111.1(3)	104.7(2)	105.4(1)
X–Sn–S(3)	155.09(6)	151.65(6)	148.80(3)
X–Sn–Y	149.21(8)	144.59(5)	146.69(3)
X–Sn–C(1)	85.8(4)	82.2(2)	82.3(1)
X–Sn–C(2)	87.7(3)	86.0(2)	83.2(1)
S(3)–Sn–Y	55.68(8)	63.70(6)	64.46(3)
S(3)–Sn–C(1)	108.5(4)	107.6(2)	109.1(1)
S(3)–Sn–C(2)	99.1(4)	104.2(2)	105.5(1)
Y–Sn–C(1)	77.3(5)	81.1(2)	85.7(1)
Y–Sn–C(2)	81.9(4)	82.9(2)	83.4(1)
C(1)–Sn–C(2)	126.1(3)	132.9(3)	134.4(1)
Sn–S(1)–C	91.2(2)	93.0(2)	96.0(1)
Sn–X–C	79.2(2)	77.8(3)	77.2(2)
Sn–S(3)–C	99.0(2)	94.8(2)	93.8(1)
Sn–Y–C	94.9(3)	77.0(3)	77.8(2)
S(1)–C–S(2)	122.8(4)	123.9(4)	123.4(3)
S(1)–C–O(1)	111.3(4)	111.4(4)	110.2(3)
S(2)–C–O(1)	124.6(5)	124.7(5)	126.4(3)
S(3)–C–S(4)	123.7(4)	124.4(4)	123.9(3)
S(3)–C–O(2)	110.3(4)	110.8(5)	110.7(3)
S(4)–C–O(2)	125.7(4)	124.8(6)	125.4(3)
C–O(1)–C	118.1(6)	119.1(5)	118.9(3)
C–O(2)–C	117.5(5)	119.2(6)	118.2(4)

the Sn···O distance of 2.950(3) Å is well below 3.7 Å, being the sum of the van der Waals radii for these atoms. The different modes of coordination of the xanthate ligands result in significant differences in the ligand parameters. Thus, the C–S(4) distance of 1.609(5) Å is significantly shorter than that for C–S(2) of 1.655(6) Å, and consequently, ΔC–S (i.e., C–S<sub>long</sub> – C–S<sub>short</sub>) for the first ligand of 0.078(9) Å is significantly less than that for the second of 0.135(9) Å. Further, there is evidence that C–O(2) is longer than C–O(1), i.e., 1.356(6) Å vs 1.322(7) Å. Angles within the respective ligands are comparable.

The coordination geometry about the tin atom in **1** is best described as being distorted trapezoidal bipyramidal with the two methyl groups being orientated over the weaker Sn–S and Sn–O interactions and defining an angle of 126.1(3)° at the tin atom. The tin atom lies 0.0897(1) Å out of the S<sub>3</sub>O plane in the direction of the methyl C(1) atom. In the lattice the closest contact between non-hydrogen atoms of 3.40(2) Å occurs between the O(1) and C(2)<sup>i</sup> atoms; symmetry operation *i*:

– *x*, –0.5 + *y*, –1 – *z*. The coordination geometry reported here for **1** is unprecedented in the structural chemistry of diorganotin bis(1,1-dithiolates).<sup>2</sup> By contrast, the structures of **2** and **3** adopt the common motif for compounds of this type.

The molecular structure of **2** is shown in Figure 2b and that of **3** in Figure 2c; selected parameters are listed in Table 1. In each of these structures both xanthate ligands are chelating but form asymmetric Sn–S distances so that each tin atom exists in a skew-trapezoidal bipyramidal geometry similar to that described above for **1**. The tin atom lies 0.0190(4) Å (0.0290(3) Å for **3**) out of the S<sub>4</sub> plane in the direction of the C(2) (C(1) for **3**) atom. The values of ΔC–S range from 0.065(9) to 0.09(1) Å in the two structures and are comparable to that found for the similar xanthate ligand in **1**. The closest non-hydrogen contact in the lattice of **2** is 3.354(7) Å and occurs between the O(1) and C(1)<sup>ii</sup> atoms; symmetry operation *ii*: +*x*, –0.5 – *y*, –0.5 + *z*. In **3**, the closest contact of 2.995(6) Å occurs between symmetry-related O(1) atoms; symmetry operation: 1 – *x*, 1 – *y*, –*z*.

The availability of three closely related structures enables a comparison of their derived interatomic parameters. There are obvious complications in making comparisons, such as the existence of a different motif for **1**; however, some interesting trends may be ascertained. The degree of asymmetry in the mode of coordination of the xanthate ligands is reflected in the ΔSn–S (i.e., Sn–S<sub>long</sub> – Sn–S<sub>short</sub>) values of 0.521 and 0.580 Å for **2**, and 0.628 and 0.540 Å for **3**. Comparing the average ΔSn–S for each structure with that found for **1** gives the following values: 0.418, 0.551, and 0.584 Å for **1–3**, respectively. This suggests an order for the Lewis acidity of the tin atom as Me<sub>2</sub>Sn > Ph(Me)Sn > Ph<sub>2</sub>Sn, i.e., opposite that expected based on electronic arguments alone. In terms of angles, the C–Sn–C angles increase from 126.1(3)° to 132.9(3)° to 134.4(1)° for **1–3**, respectively, a result that may be correlated with the increasing steric hindrance as methyl groups are successively replaced by phenyl groups. Other perturbations in the angles about the tin centers may be related to the changes in the C–Sn–C bond angles and the presence of the weakly bound oxygen atom, rather than sulfur atom, in the coordination sphere. As mentioned above, the structures reported for **2** and **3** are consistent with the predominant (S-,S-; S-,S-) motif found for R<sub>2</sub>Sn(1,1-dithiolate)<sub>2</sub> compounds.<sup>2</sup> Indeed, all of the previously reported xanthate structures, namely, Me<sub>2</sub>Sn(S<sub>2</sub>COEt)<sub>2</sub>,<sup>22</sup> Ph<sub>2</sub>Sn(S<sub>2</sub>COiPr)<sub>2</sub>,<sup>23</sup> Ph<sub>2</sub>Sn(S<sub>2</sub>COEt)<sub>2</sub>,<sup>24</sup> and Me<sub>2</sub>Sn(S<sub>2</sub>COCy)<sub>2</sub><sup>25</sup> adopt this motif. Clearly, the structure of **1** is the odd structure for the R<sub>2</sub>Sn(S<sub>2</sub>COR')<sub>2</sub> series.

Unfortunately, the compounds were not of sufficient stability to allow an examination of their solution-state structures as reported for other organotin systems.<sup>26</sup> Therefore, to ascertain the influence of intermolecular forces on the molecular geometries for **1–3**, the isolated

(22) Dakternieks, D.; Hoskins, B. F.; Tiekink, E. R. T.; Winter, G. *Inorg. Chim. Acta* **1984**, *85*, 215.

(23) Donoghue, N.; Tiekink, E. R. T. *J. Organomet. Chem.* **1991**, *420*, 179.

(24) Donoghue, N.; Tiekink, E. R. T.; Webster, L. *Appl. Organomet. Chem.* **1993**, *7*, 109.

(25) Mohamed-Ibrahim, M. I.; Khor, C.-K.; Fun, H.-K.; Sivakumar, K. *Acta Crystallogr., Sect. C* **1996**, *52*, 845.

(19) Tiekink, E. R. T.; Winter, G. *Rev. Inorg. Chem.* **1992**, *12*, 183.

(20) Collins, A. J.; Tiekink, E. R. T. *Z. Kristallogr.* **1995**, *210*, 51.

(21) Tiekink, E. R. T.; Winter, G. *J. Organomet. Chem.* **1986**, *314*, 85.



molecules have been subjected to ab initio and density functional theory molecular orbital geometry optimization calculations.

**Gas-Phase Theoretical Structures.** Previous theoretical studies comparing experimental (crystallographic) and geometry-optimized structures have employed the HF/LanL2DZ level of theory.<sup>10–12</sup> In this study, the “all-electron” Pople-type 3-21G\*\* basis set has been employed. This basis set includes polarization functions on all atoms and therefore allows for a more accurate description of the tin–ligand interactions.<sup>27</sup> Calculations were performed using the ab initio Hartree–Fock (HF), density functional (BLYP), and hybrid (B3LYP) levels of theory. The use of three distinct theoretical models was employed to test the robustness of results obtained. Indeed, an important result of this work is that the predicted relative energy ordering for **1**, **2**, and **3** does not depend on the level of theory employed. Given the adoption of two distinct structural motifs in the solid state for  $R_2Sn(S_2COMe)_2$ , all geometry optimizations were started from either the crystallographic coordinates or manufactured geometries reflecting the three combinations of the chelation modes for the xanthate ligands, i.e. (i) both ligands with S-,S-chelation, (ii) one with S-,S- and the other with S-,O-, and (iii) both with S-,O- chelation.

For the  $R = Me$  and  $Ph$  structures with either S-,S-; S-,S- or S-,O-; S-,O- chelation, the gas-phase structures are symmetric so that the  $R = Me$  compound (**1**) has very nearly  $m2m$  symmetry: one mirror plane contains the C–Sn–C fragment, the other contains Sn-( $S_2COCH$ )<sub>2</sub>, and the 2-fold axis passes through the tin atom. Two-fold symmetry, through the tin atom, was found for **3**. For the isomers with the combination of S-,S- and S-,O- chelation, the asymmetric ligand donor set precluded molecular symmetry. Symmetrization of structures, in the absence of crystal packing effects, has been noted previously.<sup>10–12</sup> Geometric parameters for the covalent interactions, collected in Table 2, tend to elongate in the gas-phase structures compared to the solid-state structures, again in keeping with expectation.<sup>10–12</sup> It is noteworthy that the geometric parameters tend to elongate depending on the level of theory chosen such that shorter distances are found for HF and the longest for BLYP calculations.<sup>10</sup>

The key result of this theoretical investigation is that regardless of the theory used, the same relative order of energies for the respective optimized structures was found, i.e.



for each of  $R_2Sn(S_2COMe)_2$ ; the theoretically predicted structures are represented in Figure 3. These energies are entirely consistent with the notion that the hard

**Table 2.** Selected Interatomic Parameters (Å, deg) for the Optimized (S-,O-; S-,O-) Structures of  $Me_2Sn(S_2COMe)_2$  (**1**),  $Ph(Me)Sn(S_2COMe)_2$  (**2**), and  $Ph_2Sn(S_2COMe)_2$  (**3**) Obtained from Ab Initio Molecular Orbital Calculations Employing the 3-21G\*\* Basis Set at the HF, B3LYP, and BLYP Levels of Theory

parameter	HF	B3LYP	BLYP
<b>1</b>			
Sn–S(1)	2.52	2.54	2.57
Sn–O(1)	2.51	2.53	2.58
S(1)–C(1)	1.74	1.74	1.76
S(2)–C(1)	1.62	1.64	1.65
C(1)–O(1)	1.38	1.42	1.44
S(1)–Sn–O(1)	60.5	60.8	60.4
S(1)–Sn–S(1)′	92.4	92.0	91.8
O(1)–Sn–O(1)′	146.5	146.4	147.0
Sn–S(1)–C(1)	90.7	91.1	91.8
Sn–O(1)–C(1)	100.4	100.1	99.8
S(1)–C(1)–S(2)	127.9	128.2	128.1
<b>2</b>			
Sn–S(1)	2.51	2.53	2.57
Sn–O(1)	2.54	2.56	2.59
S(1)–C(1)	1.74	1.74	1.76
S(2)–C(1)	1.62	1.63	1.65
C(1)–O(1)	1.38	1.42	1.44
S(1)–Sn–O(1)	60.3	60.4	60.3
S(1)–Sn–S(1)′	90.3	89.8	90.5
O(1)–Sn–O(1)′	149.1	149.2	148.9
Sn–S(1)–C(1)	91.5	92.0	92.3
Sn–O(1)–C(1)	99.9	99.5	99.7
S(1)–C(1)–S(2)	127.5	127.8	127.9
<b>3</b>			
Sn–S(1)	2.50	2.53	2.56
Sn–O(1)	2.54	2.55	2.60
S(1)–C(1)	1.74	1.75	1.76
S(2)–C(1)	1.62	1.63	1.65
C(1)–O(1)	1.38	1.41	1.44
S(1)–Sn–O(1)	60.2	60.6	60.3
S(1)–Sn–S(1)′	89.1	89.1	89.1
O(1)–Sn–O(1)′	150.6	149.7	150.4
Sn–S(1)–C(1)	91.7	91.8	92.5
Sn–O(1)–C(1)	99.9	99.7	99.7
S(1)–C(1)–S(2)	127.4	127.8	127.8

acid, tin, will form hypervalent interactions with hard donors such as oxygen in preference to soft atoms such as sulfur. Whereas a S-,O- chelation mode was found for one of the methylxanthate ligands in **1**, S-,S-chelation was found in the remaining structures, consistent with literature results. Thus, there exists a clear disparity between the experimentally observed structures and those calculated in the gas phase, at least with respect to the relative disposition of the hypervalently associated sulfur and oxygen atoms.

Relative energies for the different gas-phase structures are tabulated in Table 3. The difference in energy between the energetically favored arrangement and that of the next favored is on the order of 20 kJ mol<sup>−1</sup>, and another ca. 20 kJ mol<sup>−1</sup> separates the latter motif from the least favored geometry. However, these energy differences need to be viewed with some caution. Jonas and Frenking<sup>28</sup> have shown that the inclusion of a set of f-functions on third-row elements is often important in determining the relative energies of structural isomers. To estimate the importance of this effect on the conclusion that the S-,O-; S-,O- structures are the most stable in the gas phase, a series of single-point calcula-

(26) For example: (a) Biesemans, M.; Willem, R.; Damoun, S.; Geerlings, P.; Lahcini, M.; Jaumier, P.; Jousseau, B. *Organometallics* **1996**, *15*, 2237. (b) Jaumier, P.; Jousseau, B.; Tiekink, E. R. T.; Biesemans, M.; Willem, R. *Organometallics* **1997**, *16*, 5124. (c) Dakternieks, D.; Jurkschat, K.; Tozer, R.; Hook, J.; Tiekink, E. R. T. *Organometallics* **1997**, *16*, 3696. (d) Biesemans, M.; Willem, R.; Damoun, S.; Geerlings, P.; Tiekink, E. R. T.; Jaumier, P.; Lahcini, M.; Jousseau, B. *Organometallics* **1998**, *17*, 90.

(27) Frenking, G.; Antes, I.; Böhme, M.; Dapprich, S.; Ehlers, A. W.; Jonas, V.; Neuhaus, A.; Otto, M.; Stegmann, R.; Veldkamp, A.; Vyboishchikov, S. F. *Rev. Comput. Chem.* **1996**, *8*, 63. (b) Siegbahn, P. E. M.; Blomberg, M. R. A. *Annu. Rev. Chem.* **1999**, *50*, 221.

(28) Jonas, V.; Frenking, G. *Chem. Phys. Lett.* **1991**, *177*, 175.

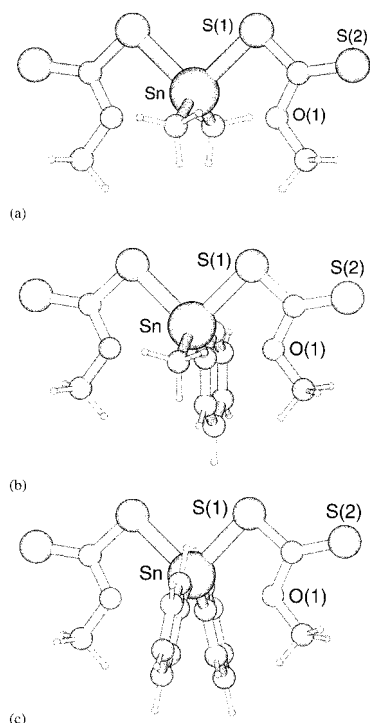


**Figure 3.** Geometry-optimized structures for (a)  $\text{Me}_2\text{Sn}(\text{S}_2\text{COMe})_2$  (**1**), (b)  $\text{Ph}(\text{Me})\text{Sn}(\text{S}_2\text{COMe})_2$  (**2**), and (c)  $\text{Ph}_2\text{Sn}(\text{S}_2\text{COMe})_2$  (**3**).

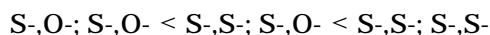
**Table 3.** Calculated Relative Energies ( $\text{kJ mol}^{-1}$ ) for  $\text{Me}_2\text{Sn}(\text{S}_2\text{COMe})_2$  (**1**),  $\text{Ph}(\text{Me})\text{Sn}(\text{S}_2\text{COMe})_2$  (**2**), and  $\text{Ph}_2\text{Sn}(\text{S}_2\text{COMe})_2$  (**3**) Employing the 3-21G\*\* Basis Set at the HF, B3LYP, and BLYP Levels of Theory (columns 2–4) and Single-Point HF/3-21G(df)<sup>a</sup> Corrections to the HF/3-21G\*\* Energies

compound	HF	B3LYP	BLYP	HF/3-21G(df)
<b>1</b> S-,O-; S-,O-	0	0	0	0
<b>1</b> S-,S-; S-,O-	+20.3	+16.3	+16.0	+1.2
<b>1</b> S-,S-; S-,S-	+43.4	+33.2	+32.1	+2.4
<b>2</b> S-,O-; S-,O-	0	0	0	0
<b>2</b> S-,S-; S-,O-	+21.8	+15.1	+16.9	+4.6
<b>2</b> S-,S-; S-,S-	+50.4	+37.1	+37.6	+12.1
<b>3</b> S-,O-; S-,O-	0	0	0	0
<b>3</b> S-,S-; S-,O-	+24.2	+18.7	+18.2	+7.1
<b>3</b> S-,S-; S-,S-	+55.2	+44.8	+42.8	+20.3

<sup>a</sup> The HF/3-21G(df) notation is used to signify that the standard 3-21G\*\* basis set has been supplemented by the inclusion of a set of d-orbitals on the oxygen atoms (with an exponent of 0.8) and a set of f-orbitals on the sulfur atoms (with an exponent of 0.55).

tions have been performed on the HF-optimized geometries for all isomers of structures **1–3**. In accord with the report of Jonas and Frenking,<sup>28</sup> the single-point calculations have been performed with a more flexible basis set that includes the addition of a set of d-orbitals on the oxygen atoms (with an exponent of 0.8) and a set of f-orbitals on the sulfur atoms (with an exponent of 0.55) to the original 3-21G\*\* basis set.

The relative energies predicted for each structure with the more flexible basis set are also included in Table 3. The first observation is that all energy differences have reduced substantially compared to the HF/3-21G\*\* energies. However, for isolated molecules **2** and **3** it is concluded that the same relative order of energies, i.e.,



is found. For isolated molecule **1**, the very small predicted energy differences calculated with the more flexible basis set do not allow a firm conclusion on the relative stabilities of each conformation.

In summary, ab initio calculations indicate for isolated molecules **2** and **3** a motif with S-,O-; S-,O- chelation is energetically preferred. Furthermore, each of these gas-phase structures is different from their experimentally observed solid-state counterparts where S-,S-; S-,S- chelation is observed. This difference quite likely indicates the role of crystal packing effects in determining molecular structure. Despite the absence of directional intermolecular forces, such as hydrogen bonding, the stabilization gained by maximizing intermolecular interactions in the crystalline phase is sufficient to induce a rearrangement of the ligand donor set. It is worth recalling here that the different ligand donor sets relate to the positions of only the weakly associated sulfur or oxygen atoms. As these are best described as hypervalent interactions, large energy differences between the isomers are not anticipated. It is also assumed that the energy barriers between the various conformations are low. In this context, it is noted that the energy associated with crystal packing found for purely organic compounds is approximately 4–8  $\text{kJ mol}^{-1}$ .<sup>29</sup>

The consequence of S-,S- chelation in the solid-state structures is to allow the presentation of the more electronegative oxygen atoms (compared with sulfur) for intermolecular interactions of the type  $\text{C-H}\cdots\text{O}$ .<sup>30</sup> A close examination of the crystal structures of **1–3** shows that indeed each oxygen atom (with the exclusion of the O(2) atom in **1**) is involved in two close (i.e.,  $< 2.95$ ) intermolecular  $\text{C-H}\cdots\text{O}$  contacts; the closest interactions were summarized earlier. It must be noted that the weakly associated sulfur atoms also participate in  $\text{C-H}\cdots\text{S}$  contacts, but these, by their very nature, must be weaker than the analogous contacts involving oxygen. Plainly, in the adoption of one motif over another for **1–3**, there is a competition between the type and magnitude of intramolecular hypervalent interactions and type and magnitude of intermolecular contacts.

## Conclusion

X-ray crystallography shows two distinct motifs for  $\text{R}_2\text{Sn}(\text{S}_2\text{COMe})_2$ , i.e., a S-,O-; S-,S- conformation for  $\text{R} = \text{Me}$  (**1**) and a S-,S-; S-,S- conformation for each of  $\text{R}_2 = (\text{Me}, \text{Ph})$  (**2**) and  $\text{R} = \text{Ph}$  (**3**). Molecular orbital calculations have been performed on the various conformations of the ligand donor sets and show that the predicted geometries are essentially independent of the level of theory employed, viz., HF, B3LYP, and BLYP. For isolated molecules **2** and **3**, the calculations predict a S-,O-; S-,O- conformation as the most stable; similar trends were found for **1**, but the energy differences are too small to draw firm conclusions. The differences between the experimental solid-state and the predicted isolated-molecule structures are ascribed to intermolecular interactions operating within the crystal lattice.

(29) Glusker, J. P.; Lewis, M.; Rossi, M. In *Crystal Structure Analysis for Chemists and Biologists*; VCH: New York, 1994.

(30) Desiraju, G. R. *Acc. Chem. Res.* **1996**, *29*, 441. Steiner, T. *Chem. Commun.* **1997**, 727. (c) Steiner, T.; Desiraju, G. R. *Chem. Commun.* **1998**, 891.

**Table 4.** Crystallographic Data for  $\text{Me}_2\text{Sn}(\text{S}_2\text{COMe})_2$  (**1**),  $\text{Ph}(\text{Me})\text{Sn}(\text{S}_2\text{COMe})_2$  (**2**), and  $\text{Ph}_2\text{Sn}(\text{S}_2\text{COMe})_2$  (**3**)

	<b>1</b>	<b>2</b>	<b>3</b>
formula	$\text{C}_6\text{H}_{12}\text{O}_2\text{S}_4\text{Sn}$	$\text{C}_{11}\text{H}_{14}\text{O}_2\text{S}_4\text{Sn}$	$\text{C}_{16}\text{H}_{16}\text{O}_2\text{S}_4\text{Sn}$
fw	363.1	425.2	487.2
cryst size, mm	$0.11 \times 0.32 \times 0.48$	$0.05 \times 0.18 \times 0.19$	$0.11 \times 0.16 \times 0.52$
color	colorless	colorless	colorless
temp, K	293	200	200
cryst syst	monoclinic	monoclinic	triclinic
space group	$P2_1$	$P2_1/c$	$P\bar{1}$
<i>a</i> , Å	6.761(1)	13.542(2)	9.376(3)
<i>b</i> , Å	7.549(2)	9.268(2)	11.952(5)
<i>c</i> , Å	13.2006(9)	14.178(2)	9.010(4)
$\alpha$ , deg	90	90	96.68(4)
$\beta$ , deg	103.256(8)	113.12(1)	97.56(3)
$\gamma$ , deg	90	90	101.18(3)
<i>V</i> , Å <sup>3</sup>	655.8(2)	1636.5(5)	971.4(7)
<i>Z</i>	2	4	2
<i>D</i> <sub>calcd</sub> , g cm <sup>-3</sup>	1.839	1.725	1.666
<i>F</i> (000)	356	840	484
$\mu$ , cm <sup>-1</sup>	25.39	20.62	17.37
transmn factors	0.975–1	0.965–1	0.940–1
no. of data coll'd	1766	4203	4763
no. of unique data	1636	4041	4490
no. of unique data with $I \geq 3.0\sigma(I)$	1490	2314	3918
<i>R</i>	0.025	0.039	0.034
<i>R</i> <sub>w</sub>	0.032	0.037	0.041
residual electron density, e Å <sup>-3</sup>	0.31	0.59	0.74

## Experimental Section

**Crystal and Molecular Structures of 1–3.** The compounds were prepared using literature methods.<sup>22</sup> Intensity data were measured on a Rigaku AFC6R diffractometer fitted with graphite-monochromatized Mo K $\alpha$  radiation,  $\lambda = 0.71073$  Å and employing the  $\omega$ – $2\theta$  scan technique. The data sets were corrected for Lorentz and polarization effects,<sup>31</sup> and an empirical absorption correction was applied in each case.<sup>32</sup> Relevant crystal data are given in Table 4.

The structures were solved by direct-methods employing SIR92<sup>33</sup> and refined by a full-matrix least-squares procedure based on *F*.<sup>31</sup> Non-H atoms were refined with anisotropic displacement parameters, and H atoms were included in the models in their calculated positions. The absolute structure of  $\text{Me}_2\text{Sn}(\text{S}_2\text{COMe})_2$  was not determined, as there were no significant differences in the refinements of the alternate structures. Final refinement details are collected in Table 4, and the numbering schemes employed are shown in Figure 2, which were drawn with ORTEP<sup>34</sup> with 50% probability ellipsoids. The teXsan<sup>31</sup> package, installed on a Silicon Graphics Iris Indigo workstation, was employed for all calculations.

**Computational Details.** All geometry optimizations were performed using the Gaussian 98 suite of programs<sup>35</sup> run on a Linux-based Beowulf commodity computing cluster<sup>36</sup> as well as a Silicon Graphics PowerChallenge supercomputer. Initial calculations were performed using the Pople-type "all-electron" 3-21G\*\* double- $\zeta$  basis set at the ab initio (Hartree–Fock), density functional (BLYP), and hybrid (B3LYP) levels of theory. Additional single-point calculations using the pre-

dicted geometries determined above were performed at the HF/3-21G\*\* level of theory with the inclusion of a set of d-orbitals on the oxygen atoms (with an exponent of 0.8) and a set of f-orbitals on the sulfur atoms (with an exponent of 0.55). All calculations were performed using default criteria for each level of theory within the Gaussian software package.

**Acknowledgment.** The Universiti Sains Malaysia and the Department of Industry, Science and Technology (Australia) are thanked for support to allow M.I.M.I. to work in Adelaide. The Australian Research Council is thanked for support of the crystallographic facility. Computing resources were provided by the South Australian Center for Parallel Computing (SACPC) and The South Australian Computational Chemistry Facility (SACCF) and are gratefully acknowledged. M.J.C. was the holder of a Science Faculty scholarship.

**Supporting Information Available:** Further details of the structure determination including atomic coordinates, bond distances and angles, and thermal parameters. This material is available free of charge via the Internet at <http://pubs.acs.org>.

OM000717V

(31) *teXsan*. Structure Analysis Software; Molecular Structure Corp.: The Woodlands, TX, 1997.

(32) Walker, N.; Stuart, D. *Acta Crystallogr. Sect. A* **1983**, *39*, 158.

(33) Burla, M. C.; Camalli, M.; Cascarano, G.; Giacovazzo, C.; Polidori, G.; Spagna, R.; Viterbo, D. *J. Appl. Crystallogr.* **1989**, *22*, 389.

(34) Johnson, C. K. ORTEP. Report ORNL-5138; Oak Ridge National Laboratory, TN, 1976.

(35) Frisch, M. J.; Trucks, G. W.; Schlegel, H. B.; Scuseria, G. E.; Robb, M. A.; Cheeseman, J. R.; Zakrzewski, V. G.; Montgomery, J. A.; Stratmann, R. E.; Burant, J. C.; Dapprich, S.; Millam, J. M.; Daniels, A. D.; Kudin, K. N.; Strain, M. C.; Farkas, O.; Tomasi, J.; Barone, V.; Cossi, M.; Cammi, R.; Mennucci, B.; Pomelli, C.; Adamo, C.; Clifford, S.; Ochterski, J.; Petersson, G. A.; Ayala, P. Y.; Cui, Q.; Morokuma, K.; Malick, D. K.; Rabuck, A. D.; Raghavachari, K.; Foresman, J. B.; Cioslowski, J.; Ortiz, J. V.; Stefanov, B. B.; Liu, G.; Liashenko, A.; Piskorz, P.; Komaromi, I.; Gomperts, R.; Martin, R. L.; Fox, D. J.; Keith, T.; Al-Laham, M. A.; Peng, C. Y.; Nanayakkara, A.; Gonzalez, C.; Challacombe, M.; Gill, P. M. W.; Johnson, B. G.; Chen, W.; Wong, M. W.; Andres, J. L.; Head-Gordon, M.; Replogle, E. S.; Pople, J. A. *Gaussian 98 (Revision A.7)*; Gaussian, Inc.: Pittsburgh, PA, 1998.

(36) Hawick, K. A.; Grove, D. A.; Coddington, P. D.; Buntine, M. A. *Internet. J. Chem.* **2000**, *3*, 4.